Electronic origins of ordering in multicomponent metallic alloys: Application to the Cu-Ni-Zn system

J. D. Althoff and D. D. Johnson
Computational Materials Science Department, MS 9161, Sandia National Laboratories, Livermore, California 94551-0969

F. J. Pinski
Department of Physics, University of Cincinnati, Cincinnati, Ohio 45221-0011

J. B. Staunton
Department of Physics, University of Warwick, Coventry CV7 4AL, United Kingdom
(Received 2 February 1995; revised manuscript received 29 August 1995)

We investigate the ordering tendencies of the fcc Cu-Ni-Zn system using a recently developed first-principles, density-functional-based theory of atomic short-range order (ASRO) in disordered substitutional alloys of an *arbitrary* number of components. We find for the binary alloys a variety of effects which should lead to competition in the ternaries: commensurate ordering (Ni-Zn), long-period ordering (Cu-rich Cu-Zn), and clustering (Cu-Ni), in agreement with experiment. We calculate the ASRO of various disordered ternary alloys (as described by the Warren-Cowley pair-correlation function) and discuss its relationship to the electronic structure of the binary and ternary disordered alloys. We find [100]-type ASRO over an extensive composition range for the ternary alloys, even though all of the ordering tendencies for binaries and ternaries have a Fermi-surface–driven component. We discuss how alloying and disorder broadening lead to these ASRO properties. For $Cu_{50}Ni_{25}Zn_{25}$, the agreement for our calculated ASRO and its indication of two ordered states at low temperature are in good agreement with experiments.

I. INTRODUCTION

Atomic short-range order (ASRO) in the high-temperature solid solution phase of metallic alloys reveals ordering tendencies that are often indicative of long-range order found at lower temperatures. Such ASRO is measurable by diffuse scattering experiments and determines many material properties at high temperature, where much materials processing takes place. Determining the underlying electronic origins of the ASRO is thus a useful enterprise, both for interpreting experiments and for predicting, understanding, and controlling the properties of alloys.

Recently, we showed that Fermi-surface nesting drives much of the ordering tendencies of the fcc Cu-Ni-Zn ternary system.[1] The present work discusses some of these results in greater detail, and also addresses the question of whether insight gained from studying various binary alloys can lead to an understanding of the ternaries. In the present work, we show that Fermi-surface nesting is, for a large portion of the ternary phase field, a unifying theme for both the fcc binaries and ternaries; however, a simple interpretation based solely on the electron-per-atom ratio ($\frac{e}{a}$) is not possible, because of the added complexity of alloy broadening of the Fermi surface, and because in a ternary alloy the composition and $\frac{e}{a}$ can be varied independently, unlike in binary systems.

Within the framework of linear-response theory, the correlation functions that describe the ASRO are related to susceptibilities of the high-temperature disordered state. Such is the inspiration of the first-principles electronic theory of compositional fluctuations in a homogeneously disordered state due to Györffy and Stocks[2,3] and Staunton, Johnson, and Pinksi[4] for binary alloys, and extended to multicomponent alloys in Refs. 1 and 5. This first-principles approach builds on the mean-field theory of ordering (the method of concentration waves) developed by Khatchaturyan.[6] It is similar to the theory of second-order transformations by Landau and Lifshitz[7] and possesses the same symmetry properties considered by Lifshitz.[8] In this paper, we apply this approach to the fcc Cu-Ni-Zn system. In particular, we investigate the two order-disorder transitions (as a function of temperature) for alloys in the vicinity of $Cu_{50}Ni_{25}Zn_{25}$.[9] In addition, we show that the three constituent binary alloy systems exhibit a rich variety of underlying electronic mechanisms, which lead to different types of chemical ordering tendencies in each and to the ordering in the ternary alloys.

While binary alloys have been widely investigated by experimental diffuse scattering techniques for years, only recently have multicomponent alloys been addressed with these approaches, and just a few alloys at that because of the added level of complexity associated with performing the experiments and interpreting the results. Currently, only two techniques are used: isotope-doped substitution requiring measurements on multiple sets of samples (of limited application, due to lack of abundance of isotopes);[10] or anomalous x-ray scattering, which tunes the x-ray energy for large contrast between constituent

0163-1829/96/53(16)/10610(16)/$10.00

species.[11] The latter technique has been used recently to determine accurately the static displacements inherent in a specific disordered alloy.[12,13] Local atomic order in a $Cu_{50}Ni_{25}Zn_{25}$ alloy has been studied both via transmission electron microscopy by van der Wegen *et al.*[14] and the anomalous x-ray scattering technique by Hashimoto *et al.*[11]

The paper is organized as follows. Section II contains a summary of the electronic theory of concentration fluctuations for an alloy of an arbitrary number of components and a discussion of Fermi-surface driven ordering. Section III contains a discussion of our results for the ASRO, the indicated low-temperature structural transformation, and their electronic origins for the fcc Cu-Ni-Zn system and related binaries. Fermi surface mechanisms are discussed, which lead to both the incommensurate and *commensurate* ordering tendencies found in the stable and metastable phases. We conclude in Sec. IV.

II. THEORY

A. Atomic short-range order in multicomponent alloys

Our first-principles theory of ASRO in multicomponent alloys has been detailed elsewhere[5] and here we give a brief summary. An arbitrary configuration of the alloy is specified by a set of occupation variables $\{\xi_i^\gamma\}$; ξ_i^γ is 1(0), if there is (is not) a γ-species atom at site i. The disordered alloy is the configurational average over all possible sets $\{\xi_i^\gamma\}$. The thermodynamic average $\langle\xi_i^\gamma\rangle$ is the site concentration (or site probability) c_i^γ, a number between 0 and 1. The $\{\xi_i^\gamma\}$ (and, therefore, the $\{c_i^\gamma\}$) satisfy a single-occupancy constraint on every site and so not all species are independent. We implement the constraint by designating the Nth species as the "host," and treating ξ_j^N as a dependent variable. There are, therefore, $(N-1)$ degrees of freedom (with regard to species) per lattice site in the N-component alloy.

A quantity that is accessible to experiment (at least indirectly) is the pair-correlation function,

$$q_{ij}^{\mu\nu} = \langle\xi_i^\mu\xi_j^\nu\rangle - \langle\xi_i^\mu\rangle\langle\xi_j^\nu\rangle \ , \tag{1}$$

which is a matrix in the species and site indices. Our theory yields a nonsingular portion of the inverse of $q^{\mu\nu}$, in reciprocal space, for the *disordered* alloy,

$$\left[q^{-1}\left(\vec{k}\right)\right]_{\mu\nu} = \left[\delta_{\mu\nu}\frac{1}{c_\mu} + \frac{1}{c_N}\right] - \beta\left[S_{\mu\nu}^{(2)}(\vec{k}) - \Lambda_{\mu\nu}\right] \ , \tag{2}$$

where β is the inverse temperature, Λ is the Onsager cavity field correction [as discussed in Refs. 4, 5, and 15], and $S_{\mu\nu}^{(2)}(\vec{k})$ is an effective chemical interaction determined from the electronic structure of the system.[5] $S^{(2)}$ embodies all electronic effects on the pair-correlation function, including electron-hole effects, and is calculated within the Korringa-Kohn-Rostoker coherent potential approximation (KKR-CPA) electronic structure scheme. Full details are given in Refs. 4, 5, and 15. In this work, we calculate $S^{(2)}$ and $\Lambda_{\mu\beta}$ for the ternary alloys within the "band-energy-only" approximation, as in Refs. 1 and 5. For the binary alloys, we quote results of both "band-energy-only" calculations of $S^{(2)}$, and $S^{(2)}$ calculations which include all terms in the local-density approximation (LDA) electronic grand potential, except displacement effects, as discussed in Refs. 4 and 15. Within this formalism, $q^{-1}(\vec{k})$ [Eq. (2)] is a nonsingular $(N-1)$-dimensional matrix in the (independent) species indices; the (discrete) translational invariance of the disordered state allows the definition of the Fourier transform. Inverting $q^{-1}(\vec{k})$ yields an $(N-1)$-dimensional portion of the $\vec{k}$-space correlation function; the remaining elements are obtained from the single-occupancy constraint and the definition of the pair-correlation function, Eq. (1).

Our equation for the inverse correlation function, Eq. (2), has the Krivoglaz-Clapp-Moss form,[16] with $[S^{(2)}(\vec{q}) - \Lambda]$ playing the role of the pairwise interaction. It is important to realize that $S^{(2)}$ incorporates on average all of the multisite, many-electron effects in the system. The "interactions" in this case, however, are determined by first principles directly and are concentration dependent, temperature dependent, and potentially long ranged. It is noteworthy that the mean-field theory of ordering becomes more exact, as the effective interactions become longer ranged.[17] Such long-ranged interactions are expected, for example, when the chemical interactions are primarily due to Fermi surface or strain effects.

Scattering experiments measure the short-range-order diffuse scattering intensity, which may be written as[18]

$$I_{\mathrm{SRO}}(\vec{k}) = \frac{1}{2}\sum_{\mu\neq\nu=1}^{N} c_\mu c_\nu (f_\mu - f_\nu)^2 \alpha_{\mu\nu}(\vec{k}) \ , \tag{3}$$

where f_μ is the (energy-dependent) scattering factor of species μ[18] and $\alpha_{\mu\nu}(\vec{k})$ is the Warren-Cowley short-range-order parameter. The Warren-Cowley short-range-order parameter, or joint probability, is related to the direct correlation function $q_{\mu\nu}$ via

$$\alpha_{\mu\nu}(\vec{k}) = \frac{q_{\mu\nu}(\vec{k})}{c_\mu\left(\delta_{\mu\nu} - c_\nu\right)} \ . \tag{4}$$

Thus, in general, only sums of the various elements of the correlation function matrix can be measured directly. From a set of measurements at $\frac{N(N-1)}{2}$ energies (i.e., wavelengths), one can determine a chosen set of $\frac{N(N-1)}{2}$ elements of the correlation function matrix $q_{\mu\nu}$.[18] The remaining elements may be determined from the single-occupancy constraint and the definition, Eq. (1) if one wishes.

At a particular wave vector $\vec{k}_0$ and at the spinodal temperature T_{sp}, element(s) of the correlation function diverge. This indicates that the homogeneously disordered state is unstable to the formation of a concentration wave of wave vector $\vec{k}_0$. This divergence occurs when (at least) one of the eigenvalues of the $S^{(2)}$ matrix is maximal, and the corresponding eigenvalue of q^{-1} van-

ishes. Corresponding to the maximal eigenvalue of $S^{(2)}$ is an eigenvector of the correlation matrix $q_{\mu\nu}$ in "composition space," and this describes the polarization of the concentration wave.[5,18,19] The presence of a nontrivial polarization differs from the case of a binary alloy, where the only possibility is species A ordering against species B. In the case of a ternary alloy, it is possible to have a partially ordered state of arbitrary polarization, for example, having pure C ordering against half A and half B (see the Appendix for more details).

B. Fermi-surface–driven ordering

It is useful to interpret the $S^{(2)}$ and α matrices in terms of the underlying electronic structure of the high-temperature, homogeneously disordered alloy. Whether a system is likely to order, on the one hand, or phase segregate, on the other, at low temperatures can be gauged from the disordered alloy's compositionally averaged density of states. By measuring the extent of the occupation of "bonding" and "antibonding" electronic states, it is usually possible to estimate whether a system will lower its energy by ordering or clustering its atoms.[20] For example, from this basis the binary systems Cu-Zn, and Ni-Zn, which we study later, are expected to order while Cu-Ni phase segregates. Having learned by these means that a given alloy is likely to have a tendency to order, the particular type of order is determined by more subtle attributes of the electronic structure.

Since (as we shall see) the specifics of the ordering tendencies of the fcc Cu-Ni-Zn system are determined by Fermi-surface properties, we now discuss the theoretical framework for Fermi-surface–driven ordering in alloys. When important distinguishing contributions to $S^{(2)}$ come from electronic structure near the Fermi level, it is illuminating to note the relationship between the $\vec{q}$-dependent contribution to $S^{(2)}$ (i.e., ignoring the species and energy dependence of matrix elements) and the quantities that describe the Fermi-surface properties as follows:[2,3]

$$S^{(2)}(\vec{q}) \sim \int d\epsilon \int d\epsilon' \ \frac{f(\epsilon) - f(\epsilon')}{\epsilon - \epsilon'} \times \int d\vec{k} \ A\left(\vec{k};\epsilon'\right) A\left(\vec{k}+\vec{q};\epsilon\right) \ . \tag{5}$$

Here, $A(\vec{k},\epsilon)$ is the Bloch spectral function (BSF),

$$A(\vec{k},\epsilon) \equiv \sum_{ij} e^{i\vec{k}\cdot(\vec{R}_i - \vec{R}_j)} \times \int d^3r \ \mathrm{Im}\left\langle G\left(\vec{r}+\vec{R}_i;\vec{r}+\vec{R}_j;\epsilon\right)\right\rangle \sim \mathrm{Im}\,\tau^c\left(\vec{k};\epsilon\right) \ , \tag{6}$$

where $\langle G(\vec{r}+\vec{R}_i;\vec{r}+\vec{R}_j;\epsilon)\rangle$ is the configurationally averaged Green's function and $\tau^c(\vec{k};\epsilon)$ is the scattering path operator,[3] both calculated within the KKR-CPA. The BSF $A(\vec{k},\epsilon)$ is the density of states at a particular $\vec{k}$ point; in a pure crystal or ordered alloy, $A(\vec{k},\epsilon)$ is a set of δ-function peaks at the band energies $\epsilon_\nu(\vec{k})$ (with band index ν). Therefore, for an ordered system, $S^{(2)}$ looks similar to a generalized susceptibility. From Eq. (5), it is clear that if the joint density of states, $A(\vec{k};\epsilon')A(\vec{k}+\vec{q};\epsilon)$, has a large value near the Fermi energy, then so too will $S^{(2)}$. The joint density of states can become large through Fermi surface nesting and/or van Hove–singularity-driven ordering. Both mechanisms are intimately tied to the shape and dimensions of the Fermi surface. Since the van Hove mechanism is only operative in $Cu_{50}Zn_{50}$ and $Cu_{25}Ni_{25}Zn_{50}$, we postpone discussion of it until the appropriate section and now discuss Fermi-surface–nesting effects.

As is evident from the presence of the factor $\frac{f(\epsilon)-f(\epsilon')}{\epsilon-\epsilon'}$ in the above equation, large contributions can typically come from energies near the Fermi energy. (However counterintuitive it may seem, this is not necessarily so, as discussed by Pinski *et al.*[20]) In a random alloy, the peaks in $A(\vec{k},\epsilon)$ are shifted and broadened by disorder. We can, however, still speak of a Fermi surface, the loci of the peak positions in $A(\vec{k},\epsilon = \epsilon_F)$, the BSF at the Fermi level, if the width of the peak in the spectral function is small compared to the dimensions of the Brillouin zone. The widths are related to the electron scattering length in the random alloy, which is responsible, for example, for the increased resistivity found in such alloys.[21] Broadening of the Fermi surface can be important in enhancing the Fermi-surface–driven ordering, as we shall see. It is worth noting that the contribution to $S^{(2)}$ will be especially large if parallel sheets exist, with large spectral weight, that are connected by a single spanning (or nesting) vector $\vec{q}_{\mathrm{nest}}$. In such a case, the energy denominator vanishes for all points on the flat, constant energy sheets of electronic structure. This results in a large contribution to $S^{(2)}$ at $\vec{q} = \vec{q}_{\mathrm{nest}}$, essentially proportional to the volume of overlap along the flat sheet attained for the particular $\vec{q}_{\mathrm{nest}}$. For a given energy, the function $A(\vec{k},\epsilon)A(\vec{k}+\vec{q}_{\mathrm{nest}},\epsilon)$ for fixed $\vec{q}_{\mathrm{nest}}$, therefore, gives an indication as to which portions of $\vec{k}$-space electronic structure give rise to ordering at a particular $\vec{q}_{\mathrm{nest}}$. Note that since $\vec{q}_{\mathrm{nest}}$ is determined by details of the electronic structure, it need not have any relationship to the underlying real-space lattice. If $\vec{q}_{\mathrm{nest}}$ is not a high-symmetry point, then the observed ASRO will be incommensurate, and the possibility of a long-period superstructure in the ordered phase exists. Although this argument is perhaps persuasive, a calculation of $S^{(2)}$ and $\alpha_{\mu\nu}$ throughout the Brillouin zone is necessary to determine the true ASRO.

To close this exposé on the relationship between possible Fermi-surface (and near-Fermi-surface) properties and features found in $S^{(2)}$, we briefly remark on the usual nomenclature of "$2k_F$" ordering when nested sheets of Fermi surface are responsible for the ordering tendencies. The $2k_F$ refers to a caliper dimension of the Fermi surface along a direction perpendicular to the parallel, flat sheets. For example, in Fig. 1(a) is the calculated Fermi surface of disordered $Cu_{75}Zn_{25}$ in the (100) plane. Notice that its Fermi surface is not perfectly flat, yet it has fairly flat features perpendicular to the [110] direc-

tion, with caliper dimension, $2k_{110}$, of 1.612 in units of $\frac{\pi}{a}$. In order to determine where the susceptibility should peak from such nesting, the usual Kohn construction[22] of drawing a circle with radius $2k_{110}$ from all symmetry related (000) points is employed. The circles which emanate from all such Bragg points will then intersect along high-symmetry lines, like X-W-X lines for an fcc phase. Given only this single energy and nesting vector, these intersecting points are ultimately where the peaks in the diffuse intensity will occur. It is these symmetry-related intersection points that are the $\vec{q}_{\rm nest}$ relevant to the above discussion, and $|\vec{q}_{\rm nest}| \approx 2k_F$. This has been used successfully, such as in CuPd,[23] CuAu,[24] and more recently Cu-Zn alloys,[25] to explain the fourfold symmetric splitting around the X points in these systems. With this background, much of the explanation involving such Fermi-surface–nesting considerations for the binaries and ternaries and its connection to experiment will be straightforward.

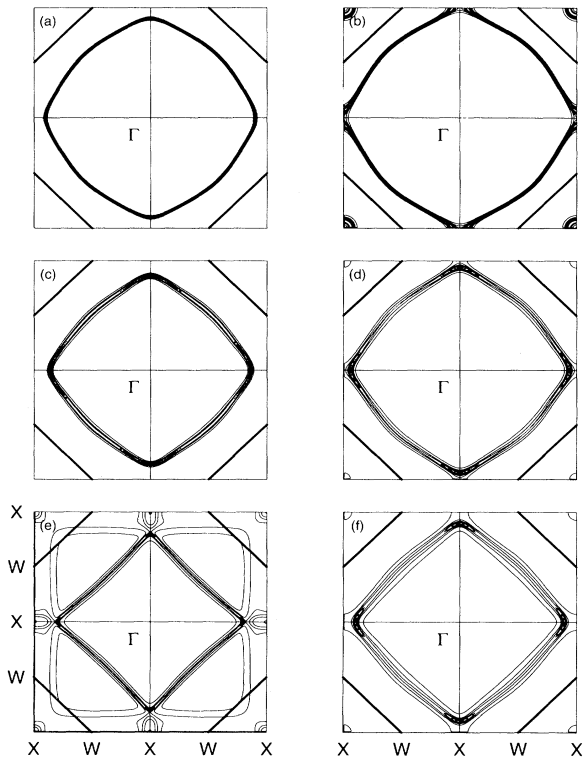

FIG. 1. Alloy Fermi surfaces in the {100} plane of the first Brillouin zone for several representatives of the homogeneously disordered Cu-Ni-Zn system, all calculated with the lattice constant 6.80 a.u.: (a) $Cu_{75}Zn_{25}$; (b) $Cu_{50}Zn_{50}$; (c) $Cu_{50}Ni_{25}Zn_{25}$; (d) $Cu_{25}Ni_{25}Zn_{50}$; (e) $Ni_{75}Zn_{25}$; (f) $Ni_{50}Zn_{50}$. Note that (a) and (d) [(c) and (f)] have the same electron-per-atom ratio, left to right is increasing Zn concentration and top to bottom is constant Zn concentration. The contours are evenly spaced between the minimum and maximum values of the spectral function to indicate the relative sharpness of the Fermi surface.

III. THE FCC Cu-Ni-Zn SYSTEM

Experimentally, the ternary fcc $Cu_{50}Ni_{25}Zn_{25}$ has been found to exhibit high-temperature short-range order and two first-order phase transitions as the temperature is decreased. Also, because both ordering and clustering tendencies have been observed in the binary alloys, the ternary may exhibit interesting competing effects, as supposed, for example, by Ceder *et al.*[26] Because the elements are neighbors in the Periodic Table, these metallic alloys should have little "charge transfer," or electronegativity, effects and we, therefore, expect the band-energy-only calculations to capture the correct ordering trends, if not fairly accurate magnitudes of the transition temperatures. For similar reasons, these alloys should have small atomic-displacement effects. Our self-consistent field (SCF-)KKR-CPA calculations confirm that the effective "charge transfer," defined in terms of the nonneutrality of atomic spheres, for the sake of discussion, is small. Diffuse scattering experiments in Cu-rich, fcc Cu-Zn alloys do, in fact, show some small displacement scattering. However, according to Vrijen *et al.*,[27] the axial ratio within the fully ordered fcc phase of $Cu_{50}Ni_{25}Zn_{25}$ is unity within experimental accuracy, confirming that lattice distortions and displacements are indeed relatively small.

At temperatures above 774 K, the $Cu_{50}Ni_{25}Zn_{25}$ alloy has a disordered $A1$ solid solution phase, which exhibits (100)-type atomic short-range order.[14,11] In fact, the individual Ni-Zn, Cu-Zn, and Cu-Ni diffuse scattering intensities have been approximately determined from anomalous x-ray scattering techniques and show that these elements of $\alpha_{\mu\nu}$ exhibit strongly ordering, weakly ordering, and clustering tendencies, respectively.[11] As the temperature is lowered, two phase transitions occur. At approximately 774 K, the alloy transforms to a partially ordered structure interpreted as having $L1_2$ symmetry in which the Zn atoms occupy one sublattice, while the Cu and Ni atoms are disordered over the remaining three sublattices. Below 598 K, a fully ordered $L1_0$ structure is stable, with the Zn atoms and Ni atoms occupying one sublattice each, while the Cu atoms occupy the other two. van der Wegen *et al.*[14] have determined these ordering occupancies for the two ordered phases through interpretation of their transmission electron microscopy results. The x-ray results of Hashimoto *et al.*[11] on the high-temperature disordered alloy cannot determine the occupation of the partially ordered state without recourse to some model.

It is also worthwhile to connect the ternary ordering behaviors and the related binary systems $Ni_{50}Zn_{50}$, $Cu_{50}Zn_{50}$, and $Cu_{50}Ni_{50}$. In these alloys, the full gamut of alloying behaviors has been observed. $Ni_{50}Zn_{50}$ goes directly from the liquid to an ordered $B2$ (bcc) structure at approximately 1300 K.[28] At approximately 1100 K, the $B2$ structure transforms into a $L1_0$ (fcc) structure, suggesting that the $B2$ phase appears mainly due to vibrational entropic effects. $Ni_{75}Zn_{25}$ is an fcc solid solution at high temperature; as the temperature is reduced, there is a two phase (fcc solid solution and ordered

$L1_0$) region very close to this composition, although the exact concentration dependence is not well characterized experimentally. $Cu_{50}Zn_{50}$ is a disordered bcc solid solution at high temperature, and transforms into an ordered $B2$ structure at approximately 770 K. Furthermore, $Cu_{75}Zn_{25}$ is an fcc solid solution, and short-range order of DO_{23}-type has been observed experimentally in the Cu-rich region.[25] The ordering tendencies are, of course, weak. In Ref. 25, the usual Fermi-surface nesting (or $2k_F$ ordering) was suggested as being responsible for the ASRO; this explanation was based on the good agreement between the suggested peak in the diffuse intensity resulting from the $2k_{[110]}$ caliper dimension [from a calculated Cu-Zn (100) Fermi surface[29]] and the actual location of the diffuse scattering intensity. $Cu_{50}Ni_{50}$ is an fcc solid solution from the liquidus down to approximately 575 K, where it phase separates. We, therefore, can characterize the equiatomic composition binaries as strongly ordering ($Ni_{50}Zn_{50}$), less strongly ordering ($Cu_{50}Zn_{50}$) (although we shall see that the hypothetical fcc phase is weakly ordering), and phase separating ($Cu_{50}Ni_{50}$).

For perspective, we review some previous theoretical work. The Fermi-surface properties of Cu-rich Cu-Zn alloys have been studied by Prasad *et al.*[29] and Stocks *et al.*[30] For the random alloys, the lattice constants and formation energies versus composition, e.g., have been studied by Johnson *et al.*[31,32] within both muffin-tin and atomic sphere approximations to the potentials. Other work has used an approximate, real-space method for studying the thermodynamic stability of $Cu_{50}Zn_{50}$, the generalized perturbation method (GPM), in conjunction with the KKR-CPA theory.[33] The KKR-CPA-GPM expands about the homogeneously disordered CPA state and obtains effective cluster interactions (ECI's) in real space that are concentration dependent. Therefore, long-range interactions, such as those involving Fermi surfaces, are inherently difficult to describe. For example, Sluiter *et al.*[33] found for Cu-rich fcc Cu-Zn solid solutions, using GPM-derived ECI's and the cluster variation method, that it was necessary to include interactions beyond fourth-nearest-neighbor in order to obtain the proper incommensurate order.[25] On the other hand, if the interactions are short ranged, then these ECI's can be combined with some form of statistical mechanics to produce phase diagrams. For example, a thermodynamic study,[34] using the KKR-CPA-GPM for the Cu-Zn binary system, indicates for $Cu_{50}Zn_{50}$ a stable $B2$ phase with T_c of 740 K [experimentally it is 730 K (Ref. 28)] and the presence of a metastable $L1_0$ phase with a T_c of approximately 288 K for $Cu_{50}Zn_{50}$; whereas, for $Cu_{75}Zn_{25}$, the calculations found a stable $L1_2$ (not the experimentally inferred DO_{23}-type) order at temperatures below about 300 K. Insight into the nature of the ASRO was not the focus of this paper and was neglected, except that one (band-energy only, muffin tin) $S^{(2)}$ calculation was given for $Cu_{80}Zn_{20}$ which showed the proper incommensurate ordering, but without examining the underlying origins.

The above experimental facts and theoretical results then suggest five questions: First, can we determine the individual diffuse intensities and their proper trends? Next, can the electronic origin of the short-range order in $Cu_{50}Ni_{25}Zn_{25}$ be ascertained? Third, is the high-temperature ASRO a precursor of the low-temperature behavior? Fourth, in the absence of an interloper phase transition, what is the only possible ground-state phase at that stoichiometry consistent with the observed (or calculated) ordering wave vector $\vec{k}_0$ (which is something that can be determined by symmetry considerations alone)? Finally, what mechanisms are responsible for the observed (or predicted) ordering behavior in the related binaries and how are they related to that found in the ternary alloys?

In what follows, we answer the above questions through calculations of atomic correlation functions $\alpha_{\mu\nu}$ (and hence the diffuse scattering) in disordered $Cu_{50}Ni_{25}Zn_{25}$ and five binaries: $Cu_{50}Ni_{50}$, $Cu_{75}Zn_{25}$, $Cu_{50}Zn_{50}$, $Ni_{50}Zn_{50}$, and $Ni_{75}Zn_{25}$. For an understanding of trends, we also study four other ternaries: $Cu_{25}Ni_{25}Zn_{50}$, $Cu_{25}Ni_{50}Zn_{25}$, $Cu_{33.3}Ni_{33.3}Zn_{33.3}$, and $Cu_{37.5}Ni_{37.5}Zn_{25}$. We restrict ourselves to only the fcc phases, even though $Cu_{50}Zn_{50}$ only has a bcc high-temperature phase with the fcc phase being metastable. Though total energy calculations for each disordered alloy may be performed (see, e.g., Johnson *et al.*,[31,32]) to obtain the appropriate lattice constants, we have chosen a lattice constant of 6.80 a.u. for the ternary (and binaries) which is very close to the 6.868 a.u. found experimentally in nearby $Cu_{47}Ni_{29}Zn_{24}$.[14] This allows us to compare directly various electronic features without the added complexity of removing the volume effects or considering two different crystal structures. Moreover, since the volume changes from the binaries to ternary are small, this is not a severe approximation. All the calculations are based on KKR-CPA potentials obtained within the atomic sphere approximation, which avoids all the problems associated with muffin-tin potentials when describing the electrostatics in the total energy, or grand potential, and the associated problems with properly describing the relative energetics of various concentration waves.[4] The local-density approximation to the density-functional theory is used as parametrized by Moruzzi, Janak, and Williams.[35] All details of performing the integrals involved in calculating $S^{(2)}$ have been discussed by Staunton, Johnson, and Pinski.[4]

It is perhaps tempting to think of the ordering tendencies and their electronic origins in a ternary alloy in terms of those in several "relevant" binary alloys. Such a scheme implies a "rigid-band" picture of the ternary and is not guaranteed to yield reliable insight. The atomic interactions in the ternary are, in general, different from those in the binaries; disorder effects, hybridization, and band-filling effects, for example, can change as one moves from a binary alloy to a ternary. Nonetheless, it is relevant to ask how the ordering tendencies of the ternary are related to those of the binary alloys of the same system. We now present a detailed study of some related fcc binary alloys and return to the ternaries afterwards.

A. Some related binary systems

1. Cu-Zn

We begin with the stoichiometric alloys $Cu_{75}Zn_{25}$ and $Cu_{50}Zn_{50}$, because (within the fcc phase) they exhibit, re-

spectively, both incommensurate and commensurate ordering. An explanation of the electronic origins of these behaviors in terms of (near) Fermi-surface properties will also be pertinent for the other alloys. Since there are recent neutron diffuse scattering data for the chemical and displacive short-range order in $Cu_{69}Zn_{31}$,[25] one can use the agreement of the calculated ASRO and our interpretation of its origin as a yardstick in the explanations which follow. Turchi *et al.*[34] have shown from KKR-CPA calculations that the fcc disordered phase is slightly higher in energy, with respect to the bcc disordered phase at 50% Zn, and, therefore, the ASRO that we calculate at 50% Zn will only be for a metastable phase.

In Fig. 2, we show a plot of the calculated diffuse scattering for $Cu_{75}Zn_{25}$ along the line X ($[100]$) to W ($[1, \frac{1}{2}, 0]$) in the Brillouin zone from the atomic short-range order only. The points are the calculated values—the squares are calculated at $T = 475$ K, the experimental quench temperature; the hexagons are calculated for the same ratio of $\frac{T}{T_C}$, i.e., the same reduced temperature, as the experiment ($\frac{T}{T_C} \approx 1.4$). The solid lines through the calculated values are a guide to the eye, and the dashed line is a reconstruction of the experimental data from the real-space short-range-order parameters given in Ref. 25. Some of the disagreement between the experimental data at $[1, \frac{1}{2}, 0]$ and the calculation comes from the additional broadening introduced in the real-space fitting procedure for the experimental data. The actual data have a sharper peak than the fit [see Fig. 2 of Ref. 25]. The fourfold symmetric peaks around (110) are centered at $\vec{q} = (1, \frac{1}{4}, 0)$ (and all symmetry-related points) and are indicative of DO_{23}-type ordering tendency. As we alluded to in the previous section, such behavior is suggestive of a Fermi-surface origin. This ASRO compares very well with the neutron diffuse scattering results of Reinhard *et al.*,[25] after removing the scattering intensity due to the small static displacements.

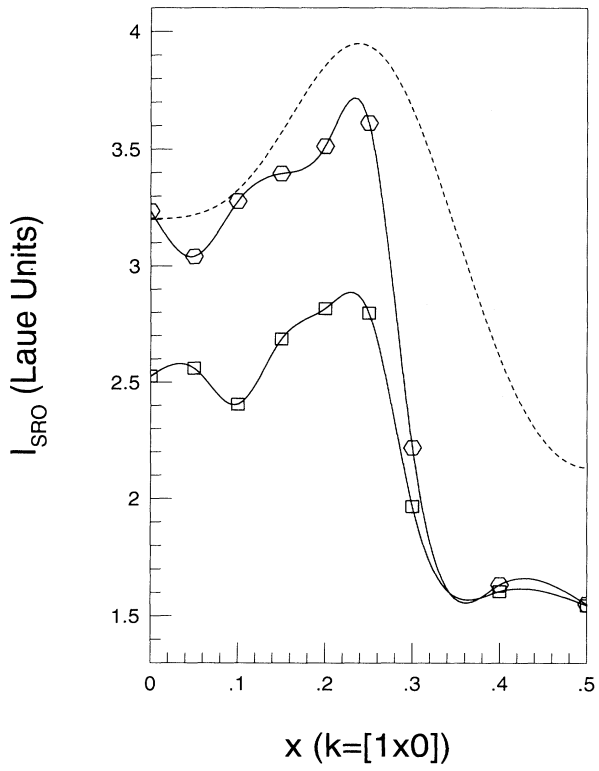

FIG. 2. Diffuse scattering intensity due to short-range order, in Laue units, for $Cu_{75}Zn_{25}$ (theory) and $Cu_{69}Zn_{31}$ (experiment) along the line $[1, x, 0]$, from X to W in the Brillouin zone. The squares are calculated at 475 K, the experimental quench temperature; the hexagons are calculated for the same value of $\frac{T}{T_C} \approx 1.4$ (reduced temperature) as the experiment. The line through the calculated values is a guide to the eye. The dashed line is the approximate experimental data, reconstructed from a real-space fit; see text.

In $Cu_{75}Zn_{25}$, the Fermi surface [i.e., $A(\vec{k}; \epsilon_F)$] is well defined on the scale of the Brillouin zone dimension, and is very similar to that of pure copper.[36] In the {001} plane, the Fermi surface, as seen in Fig. 1(a), is very similar to that obtained by Prasad *et al.*[29] and Stocks *et al.*[30] As argued by Reinhard *et al.*,[25] based on the values provided in Ref. 29, the caliper dimension across the ⟨110⟩ direction, i.e., $2k_{110}$, gives a peak at $(1, \frac{1}{4}, 0)$, etc., as in the measured total diffuse scattering intensity. Our calculated caliper dimension across the ⟨110⟩ direction has a magnitude of 1.612 (in units of $\frac{\pi}{a}$), which gives a peak at $(1, 0.736, 0)$ using the Kohn construction [very near $(1, \frac{1}{4}, 0)$, and within experimental accuracy]. Such nesting behavior along the ⟨110⟩ direction is actually enhanced due to alloying, as can be seen by the extremely flat Fermi surface in the {110} plane (this is out of the {100} plane, but along the ⟨110⟩ direction), as can be seen in Fig. 3. Thus, around the intersection of the {110} and {001} planes, there is a fairly large feature of the electronic structure in reciprocal space, which must contribute to $S^{(2)}$. Because of the obvious curvature in the Fermi surface, there cannot be perfect nesting associated with one nesting vector with magnitude $2k_{110}$, i.e., there is no one wave vector which gives a perfect overlap. As we indicated above, the actual calculations of $S^{(2)}$ find the peaks around $\vec{q}_{\text{nest}} = (1, \frac{1}{4}, 0)$, in very good agreement with the measurement and that found from $2k_F$.

Remember that to obtain these peaks at an incommensurate location within the zone, the effective chemical interactions in real space must be very long ranged,

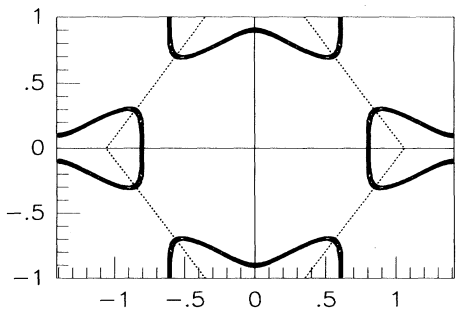

FIG. 3. Alloy Fermi surface in reciprocal space for $Cu_{75}Zn_{25}$ in the {110} plane; the horizontal zero is the {100} plane of Fig. 1(a).

as indicated by experiment.[25] We find that at least 20 shells are required to reproduce our $\vec{k}$-space calculation, while experiment[25] minimally requires 10 shells. (We fit $S^{(2)}$ to real-space coefficients to get $\alpha_{\mu\nu}$, because, unlike $\alpha_{\mu\nu}$, $S^{(2)}$ is only slightly temperature dependent and not sharply peaked; note, however, small errors in the fit of $S^{(2)}$ can easily lead to an error in the resulting fitted ASRO.) Also, we have ignored any effect of displacements, which even though small in this instance, will affect $\alpha_{\mu\nu}$, because the chemical contribution is also small. Therefore, an inversion of our approximate calculation for comparison to experimentally determined real-space interactions probably is not as fruitful as hoped in this instance. The first few calculated real-space neighbor interactions at 475 K are 20.0, −1.7, −0.11, and −0.38 meV for $Cu_{75}Zn_{25}$; for $Cu_{69}Zn_{31}$ they are 18.1, −7.4, −1.4, and −0.3 meV, from an inversion of the experimental data via the Clapp-Moss formula.[25] Since there is a 6% composition difference and $S^{(2)}$ is composition dependent, it is not clear whether the small differences are due to the composition difference or to inaccuracy from the band-energy-only approximation and neglect of displacements. Johnson *et al.* have noted that the second-nearest-neighbor, real-space interaction should be most affected by displacive effects, since this is the soft direction in fcc.[4]

As discussed very well by Reinhard *et al.*,[25] the vector $[1, \frac{1}{4}, 0]$ is indicative of DO_{23} order. Also, the streaking of the calculated (and measured) intensity along the $\langle 100 \rangle$ directions indicates that the real-space near-neighbor interactions dominate. However, since the Fermi-surface nesting gives relatively small differences among the [100], $[1, \frac{1}{4}, 0]$, and $[1, \frac{1}{2}, 0]$ vectors, all the ordered superstructures derived from these ordering wave vectors should be close in energy; for example, $L1_0$ arises from $\langle 100 \rangle$ concentration waves, DO_{22} arises from $\langle 100 \rangle$ and $\langle 1, \frac{1}{2}, 0 \rangle$ waves, and DO_{23} arises from $\langle 100 \rangle$ and $\langle 1, \frac{1}{4}, 0 \rangle$ waves. Therefore, we would "predict" a DO_{23} ground state, as did Reinhard *et al.*[25] using the experimentally derived interactions and Monte Carlo simulations. Associated with the DO_{23}-type ASRO we find $T_{sp} \approx 220$ K in the "band-energy only" approximation, including Onsager corrections (about 445 K without Onsager). This is in reasonable agreement with the 330 K transition temperature for $Cu_{69}Zn_{31}$ found from Monte Carlo simulations using the interactions found by Reinhard *et al.*[25] When charge-response (i.e., double-counting) effects are included, T_{sp} drops to about 180 K, though the ASRO still peaks at $\vec{q} = [1, \frac{1}{4}, 0]$. The Fermi-surface nesting mechanism is, therefore, robust. While charge effects tend to favor commensurate ordering and, in this case, depress the spinodal temperature, we suggest that displacements in $Cu_{75}Zn_{25}$ are also Fermi-surface driven (there is evidence for this experimentally, see Ref. 25) and may therefore push the spinodal back up. Also, the ordering tendency does become stronger with increasing Zn content (see below).

Recall that the KKR-CPA-GPM results of Turchi *et al.*[34] for $Cu_{75}Zn_{25}$ found a $L1_0$ stable ground state (instead of the experimentally inferred[25] DO_{23} ground state), using real-space interactions out to only a few near neighbors. This results, as we now see, from the interaction being very long ranged, due to the Fermi-surface nesting. In fact, Reinhard *et al.*[25] found that at least ten near-neighbor shells were required to stabilize DO_{23} relative to the simpler structures. Thus, we see, by example, the advantage of using the concentration-wave technique for addressing the ordering tendencies in various systems: it easily handles systems where the effective interactions are short ranged (as in simple clustering systems, e.g.) or long ranged (when Fermi-surface or displacement effects dominate). We do not find a $\vec{q} = (0, 0.9., 0.9)$ maximum near the spinodal temperature as did Turchi *et al.* in their muffin-tin $S^{(2)}$ calculation.[34]

We now investigate the metastable phase of fcc stoichiometric $Cu_{50}Zn_{50}$. While fcc $Cu_{50}Zn_{50}$ is not stable [Cu-Zn alloys transform to bcc at about 38% Zn (Ref. 28)], the ordering tendency and its origin are intriguing and of relevance to the ternary system. The $Cu_{50}Zn_{50}$ Fermi surface touches the Brillouin zone boundary at the X points, as shown in Fig. 1(b). Due to symmetry considerations, the BSF must always approach the Brillouin zone edge at right angles along high-symmetry lines. This is the origin of so-called van Hove singularities[36] in the density of states, for example. As a result of the average number of electrons and the disorder broadening in this system, this leads to a buildup of spectral weight around the X points; in the present case, the BSF straddles the X point. The joint density of states $A(\vec{k}, \epsilon)A(\vec{k}+\vec{q}, \epsilon)$ for $\vec{q} = (0, 0, 1)$ then has very large peaks at the X points, leading to $\langle 100 \rangle$-type short-range order. Competing with the van Hove–driven commensurate ordering is an incommensurate, Fermi-surface–driven ordering tendency (as found in $Cu_{75}Zn_{25}$), but in this case with wave vector $\vec{q} = [0, 0.15, 1]$. This is the reason why in the "band-energy-only" approximation $S^2(\vec{q})$ has similar magnitude at both $\vec{q} = [1, 0, 0]$ and $[0, 0.15, 1]$. Which is the greater varies with temperature. When Onsager corrections are included, we find a spinodal at 230 K with $\langle 100 \rangle$ order; if Onsager corrections are omitted, the spinodal is at 424 K with incommensurate $[0, 0.15, 1]$ ordering. Including charge response leads to a T_{sp} of 270 K, also with incommensurate order, but at $\vec{q} = [0, 0.4, 1]$. Since the ordered $B2$ phase occurs (experimentally) at 775 K,[28] the van Hove–driven ordering is not strong enough to overcome the established phase, especially with the larger entropy due to lattice vibration in the bcc phase. This ordering mechanism is reminiscent of the so-called van Hove singularity-driven ordering identified in stoichiometric CuPt, which is observed experimentally, and discussed in depth by Clark *et al.*[37] A similar van Hove mechanism has been cited by Staunton, Johnson, and Pinski[4] in giving rise to a predicted small secondary diffuse peak in NiPt.

2. Ni-Zn

As can be seen from Fig. 1(e), $Ni_{75}Zn_{25}$ has a very box-like Fermi surface in the (100) plane, with a nesting vector whose magnitude is less than $\sqrt{2}$ (which would lead to

⟨100⟩ commensurate ASRO). There are also flat portions of Fermi surface in the (110) plane, and these portions likewise contribute to $S^{(2)}$. The short-range order is thus incommensurate, resulting from a relatively sharp Fermi surface, with a T_{sp} of approximately 310 K from "band-energy-only" calculations with Onsager corrections (879 K without Onsager). The peak in the correlation function is broad, due to the shape of the Fermi surface—the flat pieces of Fermi surface with different nesting vectors give contributions to $S^{(2)}$ at different wave vectors. We find that the peak in the ASRO at temperatures greater than 600 K is at wave vector $\vec{k}_0 = [0, 0.19, 1]$. However, at these temperatures, the values of $S^{(2)}$ at all points around ⟨110⟩ are extremely close in energy to the value of $S^{(2)}$ at $\vec{k}_0$. Below 600 K the maximum in the ASRO shifts back and forth between two wave vectors, $[0, 0.19, 1]$ and $[0.1, 0.1, 1.0]$. When the charge response is included, the peak in the ASRO is at $\vec{q} = [0, 0.05, 1.0]$, with $T_{sp} \approx 600$ K, but the peak in the ASRO is still broad. Once again, the Fermi-surface mechanism is robust. The broadness of the peak in the ASRO may explain the experimental difficulty in actually determining the phase boundary of the two-phase region (consisting of a random solid solution plus ordered $L1_0$ $Ni_{50}Zn_{50}$), as a function of Zn composition.[28] It would be interesting to measure the diffuse intensity at this stoichiometry as a function of temperature to determine the exact nature of the ASRO.

$Ni_{50}Zn_{50}$ is the strongest ordering of the binary systems that we considered: we find ⟨100⟩ ordering with a calculated $T_{sp} \approx 1430$ K from "band-energy-only" calculations with Onsager corrections (1925 K without Onsager). Including charge-response effects lowers the spinodal to 1260 K, still at ⟨100⟩. Figure 1(f) shows a contour plot of the BSF for $Ni_{50}Zn_{50}$ in the (100) plane. The spectral function shows a relatively wider peak than that of $Ni_{75}Zn_{25}$, indicating a more disorder-broadened Fermi surface (the scattering properties of Ni and Zn are more different than those of Cu and Zn). The Fermi surface has very flat portions both in the (001) plane and the (110) plane, as in the Cu-Zn system. These flat portions are connected by an *almost* perfect $2k_F$ of $\sqrt{2}$ along the $\langle 1, 1, 0 \rangle$ direction, or a nearly perfect $\vec{q}_{nest} = [110]$, giving rise to a large value of the susceptibility at [100] and [110]. As suggested earlier, the broadness of the peak in $A(\vec{k}, \epsilon)$ makes for a larger overlap between $A(\vec{k}, \epsilon)$ and $A(\vec{k} + \vec{q}, \epsilon)$ for $\vec{q} = \vec{q}_{nest} = [1, 1, 0]$, and hence actually serves to strengthen the ordering, thereby increasing T_{sp}. Thus, nesting and the broadening due to disorder are responsible for the $L1_0$ ordering found in $Ni_{50}Zn_{50}$.

3. Cu-Ni

For $Cu_{50}Ni_{50}$, we find a $\vec{q} = (000)$ instability, i.e., clustering, with a calculated $T_{sp} \approx 564$ K, with (680 K without) Onsager corrections. The experimental miscibility gap for $Cu_{50}Ni_{50}$ is approximately 575 K. As discussed in Refs. 4 and 5, including electrostatic terms in our calculation will force charge neutrality in the case of clustering alloys, thereby decreasing T_{sp} further. Indeed, the double-counting corrections lead to a T_{sp} of about 125 K lower for the binary $Cu_{50}Ni_{50}$, in better agreement with the thermodynamic model estimates of 475 K found in the assessed phase diagram.[28] To more accurately determine this number, however, would also require the inclusion of magnetic fluctuations (see below), which we have ignored. This clustering behavior can be understood from a simple band-filling argument.

As indicated by the density of states in the disordered alloy, Fig. 4(a), the Fermi energy lies in the upper *d*-band edge of Ni and in a common *s-p* band. The density of states at the Fermi level is then largely of Ni *d*-electron character and Ni/Cu *s-p* character, which will be reflected in the character of the Fermi surface. Also, the centroids of the Cu and Ni *d* bands are relatively well separated, indicating, in tight-binding terminology, a fair amount of "diagonal" disorder; that is, $Cu_{50}Ni_{50}$ is a split-band alloy. Because of this split-band behavior in nonmagnetic $Cu_{50}Ni_{50}$, and the lack of hybridization from alloying, the filling of electronic states requires that the Fermi level lie in the antibonding Ni *d* states, as essentially found for nonmagnetic elemental Ni.[35] These states are primarily responsible for the ordering trend, and, therefore, no chemical ordering wave can lower the system's energy. (This is true if only band filling is driving the chemical ordering tendencies; however, in alloys with large split bands that do order, as in $Ni_{75}V_{25}$, $Pd_{75}V_{25}$, and $Co_{75}Ti_{25}$, electrostatics play an important role.[15]) This clustering behavior must then track the Ni portion of the DOS, as can be clearly seen in Fig. 4(b),

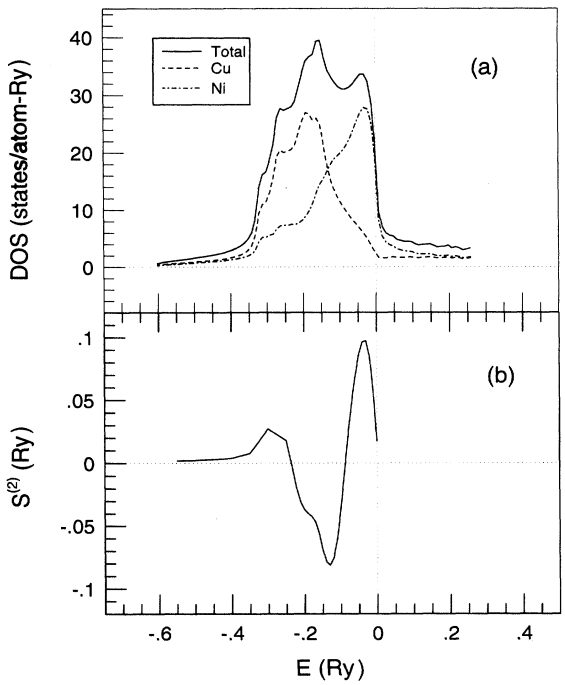

FIG. 4. (a) Electronic density of states (states/atom Ry) for disordered $Cu_{50}Ni_{50}$. (b) $S^{(2)}[\vec{q} = (000)]$ (Ry) for $Cu_{50}Ni_{50}$ as a function of energy. The vertical line is the Fermi energy.

which shows $S^{(2)}(\vec{q}=0)$ for $Cu_{50}Ni_{50}$ as a function of $(\epsilon-\epsilon_F)$, i.e., changing the electron-per-atom ratio of the alloy within a rigid-band fashion. While the alloy can lower its energy by phase separating, nonmagnetic elemental Ni cannot and should seek (for the same reasoning) a way to lower its energy through its only means: magnetic ordering, as is found in elemental Ni and Ni-rich ferromagnetic, $Cu_{50}Ni_{50}$ alloys.[28] Hence, magnetic fluctuations should also be considered for a complete description, as clustering in $Cu_{50}Ni_{50}$ can lead to small, but important, enhancements of the magnetic effects, such as superparamagnetism.[38]

Figure 5 shows a contour plot of the BSF at the Fermi energy for $Cu_{50}Ni_{50}$ in the $k_z = 0$ plane within the repeated zone scheme. The alloy Fermi surface has two distinct portions: the boxlike portion surrounding the Γ point is similar to that seen in (hypothetically nonmagnetic) "pure Ni,"[39] and is caused by a common s-p band of both Cu and Ni character; the broad portions following the zone edges are also reminiscent of the d-band contribution to the Fermi surface in "pure Ni," but they are pushed further out toward the zone edge and severely disorder broadened. (It is the band filling arising from the ternary addition of Zn that fills the remaining d bands, removing them from the Fermi surface, that will make the common s-p band play the dominant role in the ternary Cu-Ni-Zn alloys.) Because there are two disjoint portions of the BSF at this energy, the only way to achieve a sizable overlap between $A(\vec{k},\epsilon)$ and $A(\vec{k}+\vec{q},\epsilon)$ is from $\vec{q}=[000]$. This is one way to view the standard tight-binding argument that half-filled d bands favor ordering, while almost filled (empty) d bands favor clustering.[40,41] The situation is similar to that seen in PdRh,[3,4] also a clustering system, and explained by Györffy *et al.*[3] in terms of the properties of the spectral function. Note, however, that it is *not* just the properties of the spectral function in the vicinity of the Fermi level that play the dominant role here; as evident from Fig. 4(b), it is the nature of the electronic structure over a wide energy range.

Finally, because the overlap (which determined the convolution) is not a consequence of nested, flat sheets of Fermi surface, the real-space dependence of the interactions will be relatively short ranged. We find that the results for the correlation function can be fitted very well with only five nearest neighbors, as opposed to tens of near-neighbor shells for Fermi-surface-driven cases. In the band-energy-only approximation, for the first five neighbor shells our effective interactions at $T = 1294$ K are $1.65, -0.63, 0.13, 0.12, -0.01$ mRy, respectively, compared to $2.18, -1.26, -0.18, -0.10, -0.01$ mRy determined from experiment.[42] If the double-counting terms are included, the calculated effective interactions for the first five neighbor shells are $1.98, -1.02, 0.40, -0.68, -0.04$ mRy at $T = 1294$ K. We note that the interactions determined from theory are rather temperature dependent, making a detailed comparison with experiment difficult.

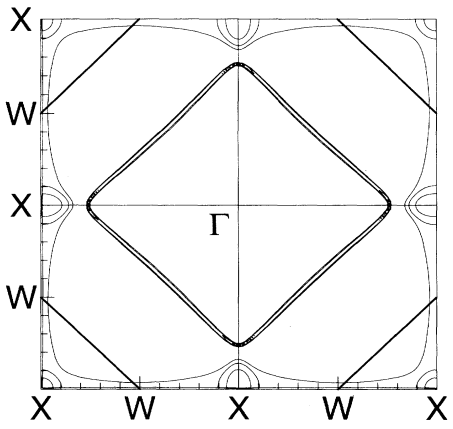

FIG. 5. Alloy Fermi surface in the first Brillouin zone for $Cu_{50}Ni_{50}$ in the {100} plane.

B. Summary of binary results

We have shown for the four binaries that Fermi-surface properties are responsible for determining a number of interesting commensurate and incommensurate ordering behaviors. The incommensurate ordering and its origins discussed for $Cu_{75}Zn_{25}$ have been observed experimentally[25] and our results agree well with that measurement and its interpretation. In $Cu_{50}Zn_{50}$, we find competition between Fermi-surface–driven, incommensurate ASRO and a van Hove singularity-driven commensurate ordering mechanism. These fluctuations lead to a metastable fcc phase, because they are relatively weak. The transition temperatures for $Cu_{50}Zn_{50}$ and $Cu_{75}Zn_{25}$ are comparable, because the nesting and van Hove mechanism are similar in magnitude in this system. The Fermi-surface nesting in stoichiometric $Ni_{50}Zn_{50}$ leads to an ordered commensurate phase (aided in part by the disorder broadening). For $Ni_{75}Zn_{25}$, the different $\frac{c}{a}$ ratio and resulting Fermi-surface dimensions lead to an incommensurate ordering peak. However, because of the shape of the Fermi surface, the fluctuations resulting from other nearby wave vectors are very close in energy, so there is not a clearcut winner and electrostatic and displacement effects may be important. The sharper Fermi surface leads to less nesting and, therefore, a lower transition temperature for $Ni_{75}Zn_{25}$ compared to $Ni_{50}Zn_{50}$. Finally, the clustering in $Cu_{50}Ni_{50}$ comes from simple band-filling requirements in a split-band alloy and the inability for that system to develop an energetically favorable ordering wave by rearranging electronic states at and around the Fermi level.

We may classify these three fcc systems, Ni-Zn, Cu-Zn, and Cu-Ni, as fairly strongly ordering, weakly ordering, and weakly clustering, respectively. The alloying effects when combining Ni, Cu, and Zn into a ternary compound will play a decisive role in determining the effective interactions arising from the electronic structure, and ultimately the ordering trends. For example (with reference to Fig. 5), ternary additions to $Cu_{50}Ni_{50}$, which increase the number of electrons in the s-p bands, will tend to enlarge the boxlike portion of the Fermi surface around the Γ point, while forcing the d-band portion along the zone

edge out of the zone. The result will be a nested Fermi surface, which should lead to an ordering tendency. We now investigate the ordering tendency and its origin in ternary fcc Cu-Ni-Zn.

C. Ordering in $Cu_{50}Ni_{25}Zn_{25}$

For the fcc ternary $Cu_{50}Ni_{25}Zn_{25}$, we find an instability to [100] ordering with a spinodal temperature of 1243 K without Onsager corrections. Onsager corrections, which require intensity sum rules to be obeyed, reduce T_{sp} to 985 K. Such corrections do not alter the origin of the transformation (yet to be discussed), but do renormalize the overall effective interactions, $S^{(2)}_{\mu\nu} - \Lambda_{\mu\nu}$, and thereby effect T_{sp}. The experimentally observed structural transition is a [100] type,[11] with a T_c of 774 K.[14] As shown in Refs. 4 and 15, and in the sections on binary alloys, inclusion of the electrostatic terms can bring the temperature scale into better agreement with experiment.

Again, we may determine unambiguously the electronic origin of the ternary ordering instability. In Fig. 6(a), we show the electronic density of states for disordered $Cu_{50}Ni_{25}Zn_{25}$ and in Fig. 6(b) the eigenvalues of $S^{(2)}(\vec{q} = \langle 100\rangle)$. Clearly, the maximal eigenvalue arising from a $\vec{q} = \langle 100\rangle$ wave peaks at the Fermi energy. From our experience with the binary alloys, this is indicative of some sort of Fermi-surface–nesting mechanism playing a role in determining the ordering tendency. In Fig. 1(c), we show a contour plot of $A(\vec{k}, \epsilon_F)$ for $Cu_{50}Ni_{25}Zn_{25}$ in the first Brillouin zone in the (100) plane. The Fermi surface is somewhat broad and boxlike, exhibiting the

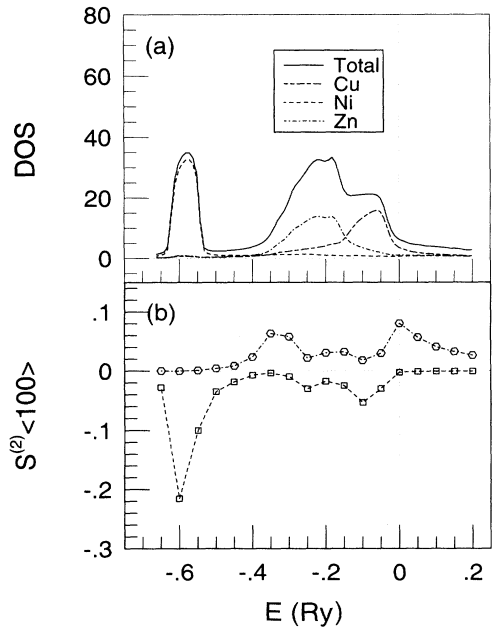

FIG. 6. (a) Electronic density of states (states/atom Ry) for disordered $Cu_{50}Ni_{25}Zn_{25}$. (b) Eigenvalues of $S^{(2)}(\vec{q} = \langle 100\rangle)$ (Ry) for $Cu_{50}Ni_{25}Zn_{25}$ as a function of energy. The vertical line is the Fermi energy.

now familiar nesting feature. Again, however, because the Fermi surface is not perfectly flat along the (110) direction (i.e., it is not a perfect square), there are several wave vectors close to $\vec{q}_{nest}$ (and energies around ϵ_F), which also contribute to the overlap $A(\vec{k}, \epsilon)A(\vec{k} + \vec{q}, \epsilon)$. This distribution of "nesting vectors" and of energies, as well as the disorder broadening, due to the differences in electronic scattering properties between Ni, Cu, and Zn, is responsible for "locking" in the perfect (100)-type ordering, similar to what was found for $Ni_{50}Zn_{50}$. Of course, the convolution, Eq. (5), does not tell the whole story, because it is species independent. It is the species dependence, obviously, that determines the ordering tendencies and the wave polarization, and these are given by the correlation functions themselves.

Normally, one expects that Fermi-surface nesting leads to a fourfold symmetric pattern near the X points [i.e., (100) and (110)] in the diffuse scattering. In fact, Hashimoto *et al.*[11] noted that the diffuse intensity *"forms a single peak without any trace of fourfold splitting, indicating the nonexistence of the so-called Fermi-surface effect often observed for the noble-metal-based short-ranged ordered alloys."* We have shown that indeed there is commensurate ASRO (i.e., no splitting of peaks) even though the specifics of the ordering are Fermi-surface driven. While obviously very unusual, it is not impossible, and it arises in this case because of nesting and disorder broadening, which increases the overlap and locks in $\vec{k}_0 = \langle 100\rangle$. It is not found, for example, due to the van Hove mechanism found in $Cu_{50}Zn_{50}$, nor due to hybridization of d states [as found in NiPt (Ref. 20)], because such states are too separated in energy to hybridize.

Does commensurate order occur for only one composition? No. In a ternary alloy it is possible to vary the composition while keeping $\frac{e}{a}$ *fixed*, in contrast to the case of binary alloys. Because the $Ni_{50}Zn_{50}$ alloying features are dominant, there should be a wide range of composition, centered around the isoelectronic line that connects $Ni_{50}Zn_{50}$ and $Cu_{50}Ni_{25}Zn_{25}$, which will also exhibit this ordering behavior. Recall, the $Ni_{50}Zn_{50}$ features will be dominant, because of the associated larger disorder from alloying and the fairly robust common s-p Fermi surface that results. Indeed, the accessed ternary diagram shows just this behavior.[43] (Although the ordering behavior must be more extensive than given in Ref. 43, because the binary $Ni_{50}Zn_{50}$ is strongly $L1_0$ and the assessed ternary phase diagram does not extend the ordered phase over that far. Reference 43 considered only the highest temperature phase, which is bcc because of entropy effects in $Ni_{50}Zn_{50}$.) In the next section, we detail some results for other ternaries.

1. *Short-range order*

We have directly compared the off-diagonal elements of the Warren-Cowley short-range-order parameter matrix in a recent letter.[1] In typical $2k_F$ ordering, we expect the nesting behavior of the Fermi surface to lead to peaks along the symmetry line X-W-X in the Brillouin zone—we, therefore, presented $\alpha_{\mu\nu}$ along that line.[1] Also, Hashimoto *et al.*[11] have explicitly plotted their measured

$\alpha_{\alpha\beta}$ along the same line. As noted, the peak is at $\langle 100 \rangle$, indicating commensurate ASRO. The Ni-Zn correlations (and hence the interactions) are the strongest and favor $\langle 100 \rangle$ ordering, the Cu-Zn correlation less strong, but still favors $\langle 100 \rangle$, and the Cu-Ni correlation of opposite (negative) sign at $\langle 100 \rangle$,[1] as observed.[11]

Quantitative comparisons between our calculated $\alpha_{\mu\nu}$ and the experimentally determined ones cannot be made for two reasons. First, the sum rules for $\alpha_{\mu\nu}(\vec{R} = 0)$ are badly violated in the experiment, which strongly affects the numerical values of $\alpha_{\mu\nu}(\vec{q})$. [Hashimoto *et al.*[11] obtain 0.8, 0.6, and 0.3 for the Ni-Zn, Cu-Zn, and Cu-Ni $\alpha_{\mu\nu}(\vec{R} = 0)$, respectively.] Within our calculation, we have examined the effect of forcing the sum rules to be so violated, and find that the overall ratios of the peak heights approach the values of Hashimoto *et al.*[11] Second, the large experimental values of $\alpha_{\mu\nu}(\vec{q} = [110])$ imply that the quench from 100 K above T_c was not rapid enough to freeze in the short-range ordered state at that temperature. For example, the value of 300 Laue units for the Ni-Zn SRO parameter is well above that typically found at such a value of $\frac{T}{T_c}$. Of course, if in our calculation we lower the temperature close to the spinodal, we also obtain large values of the Warren-Cowley parameters at [110]. Also, the sharpness of the experimental diffuse scattering peaks suggests that the system is extremely ordered, with the ASRO extending approximately 13 unit cells (estimated from the full width at half maximum of the experimental peaks). If correct, this further suggests that the internal temperature determined from the quenching process was nearer to that of the critical temperature, as indicated by our theoretical analysis.

We can thus see that due to alloying, the spinodal temperature for $Cu_{50}Ni_{25}Zn_{25}$ is lower than that of the binary $Ni_{50}Zn_{50}$. The clustering interactions within $Cu_{50}Ni_{50}$ should rapidly be dominanted by the $Ni_{50}Zn_{50}$ interactions, so that clustering should only be found in the Zn-poor ternary, as is indeed the case.[43] Furthermore, the strength of the Ni-Zn interactions would tend to force the Zn and Ni atoms to different sublattices, the Cu-Zn interactions would more weakly want Cu off the Zn sublattice, and the weakness of the Cu-Ni interactions should lead to Cu and Ni potentially occupying the same sublattice(s).

2. *Long-range order*

In the Appendix, we show that there are two long-range-order parameters ($\eta_{1,2}$), and, therefore, two phase transitions possible as a function of temperature for the $Cu_{50}Ni_{25}Zn_{25}$ alloy. Furthermore, it is shown that the most general symmetry in this [100]-type ordering system for a high-temperature, partially ordered state is a modified $L1_0$-type structure, composed of four interpenetrating simple-cubic lattices, with two sublattices always degenerate in occupancy. The exact structure is given by the polarization of the concentration wave, which in turn is determined by the system-dependent physics. For a ternary alloy, note that a modified $L1_2$-type structure is a set of measure zero in the actual solution space of $L1_0$-type structures (see the Appendix), indicating that this symmetry is a very special case. Also, we find purely from symmetry arguments that for any $L1_2$-type solution that the maximum value of the long-range-order parameter is significantly less than one.

Nonetheless, van der Wegen *et al.*[14] interpreted their TEM results as indicating that the partially ordered state of $Cu_{50}Ni_{25}Zn_{25}$ is a modified $L1_2$-type structure, in which Zn exclusively occupies one sublattice and Cu and Ni are disordered on the other three sublattices. For the occupation probability of Zn to be very close to one on one sublattice necessitates that η_1 is almost 1.0 just below the first transition, as indeed van der Wegen *et al.*[14] interpret from the TEM measurements. Clearly then these experimental results are mutually exclusive: either the system is ordered in a $L1_2$-type structure and η_1 is not near 1.0, or $\eta_1 \approx 1.0$ and the structure is $L1_0$ type. Furthermore, subsequent thermodynamic modeling,[9,14] using the cluster variation method, considered only an $L1_2$-like state at high temperatures, not a general $L1_0$-like state. We now discuss our results and a possible resolution of this conundrum.

As shown in the Appendix, and discussed in detail in Ref. 5, the eigenvector of $q^{-1}_{\mu\nu}$ corresponding to the maximal eigenvalue (which causes the divergence of the correlation function) determines the occupation probability of the partially ordered state, or, in particular, the polarization of the concentration wave. The partially ordered state found from this eigenvector is a modified $L1_0$-type structure, where on one of the four simple cubic sublattices the probability for finding a Zn atom is strongly enhanced, and on the other three sublattices it is reduced. In fact, our mean-field estimate for the Zn-enhanced sublattice is $c^I_{\mathrm{Zn}} = 0.25 + (0.57)\eta$, and the other single-particle distributions are described fully in Table I. Of course, it follows that on the Zn-enhanced sublattice, the probability for finding a Cu atom or a Ni atom is reduced; whereas, on the Zn-depleted sublattices, the probability for finding a Cu or Ni atom is enhanced. Symmetry alone dictates that two of the sublattices are identical. The structure is, therefore, layered; the two identical sublattices constitute a single layer, and the other layer comprises two different sublattices. The structure is, therefore, tetragonal—the layer stacking de-

TABLE I. Atomic distribution function in real space of the state to which the high-temperature homogeneously disordered state is unstable at T_c. η is the long-range-order parameter.

Component	Sublattice	Probability
n^{Zn}	1	$0.25 + 0.57\eta$
n^{Zn}	2	$0.25 - 0.48\eta$
n^{Zn}	3,4	$0.25 - 0.045\eta$
n^{Ni}	1	$0.25 - 0.51\eta$
n^{Ni}	2	$0.25 + 0.43\eta$
n^{Ni}	3,4	$0.25 + 0.04\eta$
n^{Cu}	1	$0.5 - 0.06\eta$
n^{Cu}	2	$0.5 + 0.05\eta$
n^{Cu}	3,4	$0.5 + 0.005\eta$

fines a preferred direction. Of course, this is not quite the $L1_2$-type occupation interpreted experimentally.[14] However, if small domains of $L1_0$-type, ordered unit cells exist and are averaged over the three possible tetragonal orientations, then we see that this would appear to TEM measurements exactly as $L1_2$-type occupation, as van der Wegen *et al.*[14] claim. As a result, it is possible that the TEM results are showing an average over domains of an $L1_0$-type state with different tetragonal orientations and, therefore, implying an $L1_2$-like state. Of course, high-resolution TEM experiments would be able to decide between these two possibilities by focusing on single domains. It is worth commenting that the $L1_0$-like partially ordered state that we find is "nearby" in solution space to the single point where the $L1_2$-like state occurs, in the sense that the two identical sublattices of the $L1_0$-like structure are almost completely random (see Table I). It is this property that leads to a conclusion similar to that of van der Wegen *et al.*, if one considers averaging over the tetragonal orientations.

As noted above, in an fcc ternary alloy, the concentration-wave approach for $\vec{q} = [100]$ only allows for a fully ordered $L1_0$ structure at $T = 0$. Since the above noted partially ordered $L1_0$ structure has different occupation probabilities than those of the ground-state $L1_0$ structure, a second phase transition at lower temperature to a fully ordered $L1_0$ structure can take place. Provided an instability to some other partially ordered structure (not the [100] type as found above) does not preempt this transition, it will occur. Given that the ternary $Ni_{50}Zn_{50}$ interactions are relatively strong and originate from a Fermi-surface mechanism, there should be no such interloper phases and the $L1_0$ structural phase transition must occur.

Since our discussion is based on the stability of the high-temperature disordered state, we are not able to predict (based on the eigenvector, etc., already calculated) the temperature for this second transition. However, one simple estimate can be made. From the occupation probability distribution (see the Appendix), we know that the transition must occur before any probability becomes less than zero on any one of the sublattices. Because the transition temperature is roughly proportional to ΔE_{order}, or η^2, then T_{sp}^{II} is $(1-\eta^2)T_{\text{sp}}^{I}$, since the coefficients in the Landau expansion are the same. An $\eta = 0.49$ is found to make one of the Cu/Ni sublattices have a negative occupancy; therefore, the long-ranged-ordered state with $L1_0$ symmetry must occur at about $T_{\text{sp}}^{II} = 0.76T_{\text{sp}}^{I}$. From the experimental temperatures of 774 K and 623 K for the transitions I and II,[27] $T_{\text{sp}}^{II}/T_{\text{sp}}^{I}$ is 0.80, close to the estimate of 0.76.

D. Other ternary alloys

We have seen that Fermi-surface nesting drives much of the ordering tendencies for $Cu_{50}Ni_{25}Zn_{25}$ and several binaries of the Cu-Ni-Zn system. Since the Fermi-surface dimensions depend on the electron-per-atom ratio ($\frac{e}{a}$), we expect (to a first approximation) the ordering wave vector to depend likewise on $\frac{e}{a}$. The position of the peak in the short-range-order parameter can further be modified somewhat by the changing degree of disorder broadening. The changes in shape of the Fermi surface as $\frac{e}{a}$ is changed will affect both the strength of the ordering (as reflected in T_{sp}) and, potentially, the ordering wave vector. For each alloy, we calculate the Warren-Cowley short-range-order parameter $\alpha_{\mu\nu}$ and the Bloch spectral function $A(\vec{k}, \epsilon)$. Comments concerning the ASRO are based on the calculations of α; comments concerning the Fermi surfaces are based on the calculations of $A(\vec{k}, \epsilon)$. All calculations have been performed at the same lattice constant used for $Cu_{50}Ni_{25}Zn_{25}$.

The results which follow were summarized as a Gibbs triangle of the Cu-Ni-Zn system in Ref. 1. The line joining pure Cu with binary $Ni_{50}Zn_{50}$ is the Cu-isoelectronic line; along this line all alloys are isoelectronic with pure Cu. $Cu_{50}Ni_{25}Zn_{25}$ lies on this line, as does $Ni_{50}Zn_{50}$ and the ternary $Cu_{33.3}Ni_{33.3}Zn_{33.3}$. All along this line we find $\langle 100 \rangle$ ASRO. Since $\frac{e}{a}$ is constant, we expect the magnitude of the nesting vector to remain approximately constant, and this is why the ordering wave vector does not change. The curvature of the Fermi surface changes as does the disorder broadening, changing the size of the nested portions and effecting T_{sp}. On the Cu-isoelectronic line, we find $\langle 100 \rangle$ ASRO for $Cu_{33.3}Ni_{33.3}Zn_{33.3}$, with a spinodal temperature of 1160 K (1500 K without Onsager corrections), slightly higher than that for $Cu_{50}Ni_{25}Zn_{25}$.

As we change $\frac{e}{a}$, the nesting vector changes. For example, for $Cu_{75}Zn_{25}$, the nesting mechanism leads to incommensurate order (on an fcc lattice) with $\vec{q} = (1, \frac{1}{4}, 0)$. The ternary alloy $Cu_{25}Ni_{25}Zn_{50}$ is isoelectronic with $Cu_{75}Zn_{25}$, and the Fermi surface dimensions lead to a similar nesting vector. However, the disorder broadening of the Fermi surface actually leads to a larger value for the joint density of states at $\vec{q} = \langle 100 \rangle$, as a result of van Hove singularities [see Fig. 1(d)]. Therefore, because of disorder broadening, which pushes the spectral weight to high-symmetry points, the ASRO for $Cu_{25}Ni_{25}Zn_{50}$ actually turns out to be *commensurate*. The peak in the ASRO is broad, as might be expected in such a case. The spinodal temperature is 950 K (1575 K without Onsager corrections). It should be pointed out that the Zn-rich end of the phase diagram is experimentally bcc, and studies of the fcc-bcc transition are a subject of ongoing work.

Similarly, although $Cu_{37.5}Ni_{37.5}Zn_{25}$ has a value of $\frac{e}{a}$ which is different from that of pure Cu, it too shows $\langle 100 \rangle$ ASRO with a T_{sp} of 875 K (1180 K without Onsager corrections), also due to alloying effects on the Fermi surface properties. Ultimately, as $\frac{e}{a}$ continues to change, and likewise the Fermi surface dimensions, disorder broadening can no longer lock in the commensurate ASRO and the ordering tendencies become incommensurate. Thus, as discussed above for the binary alloy $Ni_{75}Zn_{25}$ and, as discussed in Ref. 1, we find incommensurate ASRO for $Cu_{25}Ni_{50}Zn_{25}$. For this ternary, several wave vectors compete as the temperature is lowered. Including Onsager corrections, we find a spinodal at 485 K with ordering wave vector $(0, 0.1, 1.0)$. If Onsager corrections are omitted, the spinodal is at 1005 K, with ordering

wave vector $(0, 0.05, 1.0)$. The rough boundary between commensurate and incommensurate order that we find is in very good agreement with the compiled data of Thomas.[43]

IV. SUMMARY AND CONCLUSION

We have applied the first-principles theory of ASRO in multicomponent alloys to the ternary Cu-Ni-Zn system. For $Cu_{50}Ni_{25}Zn_{25}$, the Warren-Cowley parameter and the partially ordered state at high temperatures and the ultimate ground-state configuration were found. Ordering transitions and their relative trends were also reproduced. The electronic origin of this ordering behavior was found to be arising in part from a (at and near) Fermi-surface mechanism even though commensurate ordering (i.e., no fourfold splitting) was found. Indeed, this one single, electronic mechanism is responsible for selecting the type of ordering behavior in the entire fcc portion of the Cu-Ni-Zn ternary, a rather remarkable feature. Only in the very Zn-poor region of the ternary phase diagram can the interactions be short ranged, in contrast to the short-ranged interactions supposed by Ceder *et al.*[26] in their ground-state search for $Cu_{50}Ni_{25}Zn_{25}$ and other similar competing-type systems. In general, the results of this mean-field theoretical approach are very impressive for a Gorsky-Bragg-Williams-like model, because of the more sophisticated and robust Hamiltonian and the physics contained therein. The power of this first-principles method of determining ASRO is not only to help interpret experimental diffuse scattering in multicomponent alloys, but also reveal the electronic mechanisms that are playing a role in the ordering tendencies found in the high-temperature states. This latter information is difficult to obtain from total energy calculations in combination with statistical mechanics methods, for example, and, as such, it would be highly advantageous to use both of these complementary approaches.

ACKNOWLEDGMENTS

This work was supported by the U.S. Department of Energy, Office of Basic Energy Sciences, Division of Materials Science through a New Initiative under Contract No. DE-AC04-94AL85000, by NSF under Contract No. DMR 9217297, and by the Engineering and Physical Sciences Research Council, U.K. We also thank Lee Robertson for helpful discussions regarding the diffuse scattering data in the Cu-Ni-Zn ternary.

APPENDIX: CONCENTRATION WAVES IN Cu_2NiZn

We discussed the concentration-wave formalism for a ternary alloy in detail in Ref. 5 and here we focus on the results for $\langle 100 \rangle$ ordering of a ternary alloy on an fcc lattice. The atomic distribution function is an $(N-1)$-dimensional vector in the species indices (i.e., in "concentration space"), each component $n_\gamma(\vec{r}_i)$ representing the probability for finding an atom of species γ at location $\vec{r}_i$. In what follows, we take the independent species to be species A and B, with species C the "host." At each site i, the components of the distribution function sum to one, reflecting the single occupancy constraint.

As discussed in Ref. 5, our theory of ASRO in disordered alloys can be interpreted in terms of a generalized Gorsky-Bragg-Williams (GBW) model. A stability analysis of the related GBW model leads to the same spinodal temperature implied by the divergence of the pair correlation function and further leads to a concentration-wave interpretation of the SRO and LRO. Such a stability analysis requires the examination of the free energy in the quadratic approximation,

$$F = F_0 + \sum_{\alpha\beta} \sum_{\vec{k}} c^\alpha \left(\vec{k}\right) \mathcal{F}^{\alpha\beta} \left(\vec{k}\right) c^\beta \left(\vec{k}\right) , \qquad \text{(A1)}$$

where F_0 is the free energy of the reference state of interest (in our case, the random alloy) and $\mathcal{F}$ is the so-called free-energy quadric, which is related to the inverse of the pair-correlation function. As discussed in Ref. 5, we can write the atomic distribution function as an expansion in the principal directions in concentration space of the free-energy quadric $\mathcal{F}$.[5,44] These principal directions play the role of "normal concentration modes:" the instability of the homogeneously disordered state arises from a vanishing of the restoring force against creating a concentration wave corresponding to a "soft mode." At the spinodal, the free-energy cost to create a concentration modulation whose polarization in concentration space is described by the "soft mode" is zero.

As discussed by de Fontaine,[44] the original concentration space of a ternary alloy, which he calls the "Gibbs composition space," is an equilateral triangle and hence an oblique space: axes chosen along the directions of increasing atomic concentration are not mutually perpendicular. To obtain the principal directions of the free-energy quadric, it is necessary to transform from the Gibbs space to Cartesian coordinates. Such a transformation preserves the value of the quadratic form in Eq. (A1) and is not orthogonal, reflecting the oblique nature of the Gibbs space. The principal directions x_σ of the free-energy quadric are then the eigenvectors of the matrix $\mathcal{F}_x = O^T \mathcal{F} O$, the free-energy quadric transformed into Cartesian coordinates (the superscript T denotes matrix transpose). These principal directions are *independent* of the choice of host species. These eigenvectors are transformed back into the Gibbs composition space according to $c^\alpha = \sum_\sigma O_{\alpha\sigma} x_\sigma$, for use in the concentration-wave formalism, as described below. It is thus the oblique transform O that carries the information of which atomic species are chosen to be the independent variables. Note that the eigenvectors in the (oblique) Gibbs composition space are, in general, not orthogonal. The final description of the concentration wave is of course independent of the choice of host.

The free-energy quadric in Cartesian space ($\mathcal{F}_x$) is a symmetric matrix and has orthogonal eigenvectors. For a ternary alloy, the matrices are of dimension 2. If we

choose the eigenvectors to be normalized there is thus, for the case of a ternary alloy, only one parameter that describes the eigenvectors of $\mathcal{F}_x$. We can, therefore, write the eigenvectors for either matrix as

$$\begin{bmatrix} e_1^A(\vec{k}) \\ e_1^B(\vec{k}) \end{bmatrix} = \begin{bmatrix} \sin\theta_{\vec{k}} \\ -\cos\theta_{\vec{k}} \end{bmatrix} \; ; \; \begin{bmatrix} e_2^A(\vec{k}) \\ e_2^B(\vec{k}) \end{bmatrix} = \begin{bmatrix} \cos\theta_{\vec{k}} \\ \sin\theta_{\vec{k}} \end{bmatrix} , \tag{A2}$$

where A, B are Cartesian axis labels. The parameter θ is determined by the interactions and plays the role of a "polarization angle" for the concentration wave of wave vector $\vec{k}$. The polarization angle determines the occupations of the sites that are (potentially) made inequivalent by the concentration wave, and is itself determined by the interactions. For a ternary alloy, in contrast to the case of a binary, the interactions determine not only the ordering wave vector and spinodal temperature, but the polarization angle as well. We shall take $\theta_{\vec{k}}$ to be the parameter which describes the eigenvectors of $\mathcal{F}_x$ in all that follows. As stated above, it is necessary to find the eigenvectors of $\mathcal{F}_x$ (in the Cartesian space) and transform them back to the Gibbs space to obtain a set of "normal concentration modes" in which to write the concentration waves. The normal concentration modes are not necessarily orthogonal (because the transformation O is oblique), but they can of course still be described by the single parameter θ—the components are linear combinations of $\sin\theta$ and $\cos\theta$ with coefficients that are matrix elements of O.

We write the atomic distribution function as an expansion in the normal concentration modes as follows:

$$\begin{bmatrix} n^A(\vec{r}) \\ n^B(\vec{r}) \end{bmatrix} = \begin{bmatrix} c^A \\ c^B \end{bmatrix} + \sum_{s,\sigma} \eta_\sigma^s \begin{bmatrix} v_\sigma^A\left(\vec{k}_s\right) \\ v_\sigma^B\left(\vec{k}_s\right) \end{bmatrix} \times \sum_{j_s} \gamma_\sigma\left(\vec{k}_{j_s}\right) \exp(i\vec{k}_{j_s}\cdot\vec{r}) , \tag{A3}$$

where $v_\sigma^{A,B}(\vec{k}_j)$ are the A, B components of the normal concentration modes for the σth branch, as described above, and η_σ^s is the order parameter for the σth branch and sth star. The first sum is over branches σ and stars s; the second over j_s, the vectors making up the sth star. The $\gamma_\sigma(\vec{k}_{j_s})$ are coefficients determined by symmetry; we use the convention that for all $\eta_s^\sigma = 1$, Eq. (A3) describes a perfectly ordered state. For the case of interest here, there is one relevant star, the $\langle 100\rangle$ star, comprised of the vectors [100], [010], and [001]. Since there is one star and $\mathcal{F}$ is a 2×2 matrix, there are two order parameters in the expansion (A3), and hence two order-disorder transformations are possible as the temperature is lowered from the homogeneously disordered state.

As discussed in the text, the correlation function $q_{\mu\nu}(\vec{k}, T)$ for the homogeneously disordered state diverges for some wave vector $\vec{k}_0$ at the spinodal temperature $T_{\rm sp}$. In the context of concentration waves, this means that at least one of the order parameters in Eq. (A3) becomes nonzero—the homogeneously disordered state is absolutely unstable against the formation of a concentration wave of wave vector $\vec{k}_0$. Also, the instability temperature, i.e., the spinodal, is often very close to the actual transition temperature if the transition is first order.[6]

A $\langle 100\rangle$ ordering wave on an fcc lattice divides the structure into four interpenetrating simple-cubic sublattices. At $T = 0$, the structure must be fully ordered—all of the $n_\alpha(\vec{r})$ must be either zero or one. For any temperature, the system of Eq. (A3) may be inverted to give the $\{c_\alpha\}$ and the $\{\gamma_\sigma(\vec{k}_{j_s})\}$ in terms of the $\{n_\alpha(\vec{r})\}$. By examining this solution of (A3) (in particular for the $\{c_\alpha\}$) one finds that the only stoichiometry that can sustain a *ternary* ordered phase at $T = 0$ is ABC_2. The structure has a modified $L1_0$ symmetry with species A predominantly occupying the corners of the fcc cube, species B predominantly occupying opposite face centers of the fcc cube, and species C predominantly occupying the remaining face centers, the central plane of the fcc cube. The C species occupies two of the four interpenetrating simple cubic sublattices—those two sublattice occupations are equivalent and must remain so as the temperature is raised. From the inversion of (A3) at $T = 0$, one also obtains the temperature-independent parameters $\{\gamma_\sigma(\vec{k}_{j_s})\}$ in terms of the eigenvector components.

In a partially ordered state, i.e., one described by Eq. (A3) with only one of the two long-range-order parameters nonzero and the other zero, the symmetry of the superstructure described by $\vec{k} = \langle 100\rangle$ is determined by the corresponding eigenvector. When only one order parameter is nonzero, the structure is still, in general, $L1_0$-like; however, for one *specific* value of the eigenvector components, three sublattices are equivalent and the structure has $L1_2$ symmetry. This is obviously a rather special situation. Furthermore, the probability distribution that results for only one long-range-order parameter nonzero places stringent limits on the maximum value that that order parameter may take. This maximum value of the order parameter in an fcc $\vec{k} = \langle 100\rangle$ partially ordered state is plotted in Fig. 7 as a function of the polarization angle in the Cartesian space. We emphasize that this result is based on symmetry alone, and not on any of our approximate electronic structure results. The experimentally inferred $L1_2$ phase occurs at $\theta = \frac{\pi}{2}$; our theoretical value is $\theta = 0.36\pi$. The situation is similar to Khachaturyan's discussion of nonstoichiometric phases in binaries[6]—the probability distribution for certain values of the eigenvector components takes on negative values for values of the order parameter greater than some maximum value, which is generally less than one. These are then phases that are not stoichiometric for the ternary. In particular, for the partially ordered phase of $L1_2$ symmetry the maximum value of the order parameter is $\eta_{\rm max}^{L1_2} = \frac{2}{3}$, leading to a maximum value for $n_{1,\rm max}^{\rm Zn} = \frac{3}{4}$. Last, we note that *any* phase with one of the long-range-order parameters equal to zero cannot exist at $T = 0$ by Nernst's theorem, and there must be a second phase transition to a state, which does satisfy Nernst's

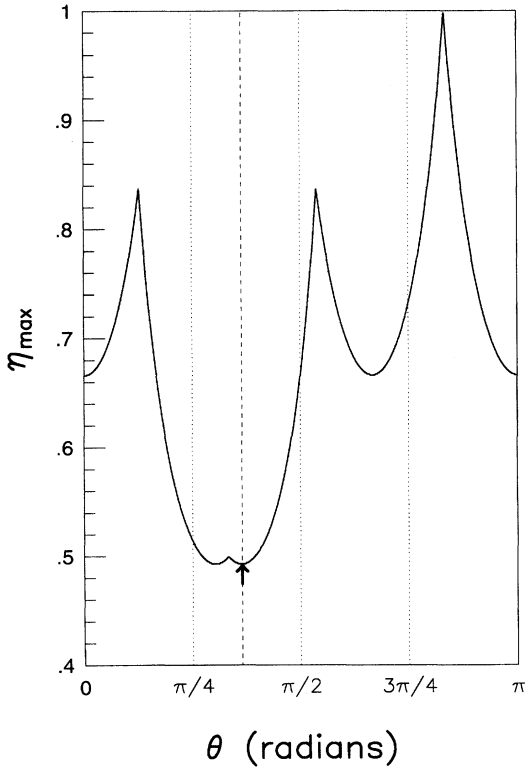

FIG. 7. The maximum possible value of the order parameter in the partially ordered state as a function of the polarization angle in the Cartesian space. The experimentally inferred $L1_2$ state occurs at $\theta = \frac{\pi}{2}$; our theoretically determined state occurs at $\theta = 0.36\pi$, indicated by the dashed line and arrow.

theorem.

The normal concentration modes near the ⟨100⟩ ordering instability at $T = 1000$ K are shown in Table II (the instability occurs at $T_{sp} \approx 985$ K). The mode for which the free-energy cost is lowest and which causes the divergence in $q_{\mu\nu}$ is that corresponding to mode 2. Upon substitution into Eq. (A3), taking into account the solution for the parameters $\gamma_\sigma(\vec{k}_{j_s})$ in terms of the eigenvectors of $\mathcal{F}$, and setting the long-range-order parameter $\eta_1 = 0$, one obtains the atomic distribution function $n(r)$ shown in Table I. The distribution function describes a three sublattice superstructure, as discussed previously.

TABLE II. Normal concentration modes in Gibbs space near the spinodal temperature. The independent species here are zinc (A) and nickel (B).

Component	Eigenvector 1	Eigenvector 2
e_A	0.476 75	1.051 68
e_B	0.672 41	-0.938 72

A few comments are in order. First, although it may appear as if some of the probabilities go negative, this is not the case. This distribution function is only valid for small values of the long-range-order parameter η_2; η_2 is temperature dependent and is only equal to one at $T = 0$. Because the symmetry of the partially ordered phase is not that of the fully ordered phase ($\eta_1 = \eta_2 = 1$), there must be a second phase transition at some nonzero temperature. The second phase transition must occur before any of the components of $n(\vec{r})$ become negative. Further, the eigenvectors of $S^{(2)}$ are computed for the homogeneously disordered state, and, therefore, are approximate; hence, $n(\vec{r})$ is only indicative of the nature of the long-range order present at temperatures just below the phase transition, but it is not a completely quantitative description. Finally, our eigenvectors correspond to a distribution function that describes a state in which the probability for finding zinc on one sublattice is greatly enhanced; on that same sublattice, the probability for finding copper or nickel is decreased. On the other two sublattices, the probability for finding zinc is decreased, and the probability for finding copper and nickel is enhanced. This distribution function describes a partially ordered, tetragonal, $L1_0$-like structure, that, in particular, has two sublattices within a plane almost random Cu and Ni (see text for discussion and comparison to experiment).

[1] J.D. Althoff, D.D. Johnson, and F.J. Pinski, Phys. Rev. Lett. **74**, 138 (1995).

[2] B.L. Györffy and G.M. Stocks, Phys. Rev. Lett. **50**, 374 (1983).

[3] B.L. Györffy *et al.*, in *Alloy Phase Stability*, edited by G.M. Stocks and A. Gonis (Kluwer, Dordrecht, 1989), p. 421.

[4] J.B. Staunton, D.D. Johnson, and F.J. Pinski, Phys. Rev. B **50**, 1450 (1994).

[5] J.D. Althoff and D.D. Johnson (unpublished).

[6] A. Khachaturyan, *Theory of Structural Transformations in Solids* (Wiley, New York, 1983).

[7] L.D. Landau and E.M. Lifshitz, *Statistical Physics, Part 1*, 3rd ed. (Pergamon Press, New York, 1980).

[8] E. M. Lifshitz, Fiz. Zh. **7**, 251 (1942).

[9] A. De Rooy, G.J.L. van der Wegen, P.M. Bronsveld, and J.Th.M. De Hosson, Scr. Metall. **15**, 1362 (1981).

[10] P. Cenedese, F. Bley, and S. LeFabvre, Acta Crystallogr. Sec. A **40**, 228 (1984).

[11] S. Hashimoto *et al.*, J. Phys. Soc. Jpn. **54**, 3796 (1985).

[12] G. Ice *et al.*, Phys. Rev. Lett. **68**, 863 (1992).

[13] C.J. Sparks, G. Ice, L. Shaffer, and J. Robertson, in *Metallic Alloys: Experimental and Theoretical Properties*, edited by R. Jordon and J. Faulkner (Kluwer, Boston, 1994), p. 73.

[14] G.J.L. van der Wegen, A. De Rooy, P.M. Bronsveld, and J.Th.M. De Hosson, Scr. Met. **15**, 1359 (1981).

[15] D.D. Johnson, J.B. Staunton, and F.J. Pinski, Phys. Rev. B **50**, 1473 (1994).

[16] M. Krivoglaz, *Theory of X-Ray and Thermal-Neutron Scattering by Real Crystals* (Plenum Press, New York, 1969).

[17] V.G. Vaks, A.I. Larkin, and S.A. Pikin, Zh. Eksp. Teor. Fiz. **51**, 361 (1966) [Sov. Phys. JETP **24**, 240 (1967)].

[18] D. de Fontaine, *Solid State Physics: Advances in Research and Applications*, edited by D. Turnbull, F. Seitz, and H.

Ehrenreich (Academic, New York, 1979), Vol. 34, p. 73.
[19] D. Badalyan, A. Khachaturyan, and A. Kitaigorodskii, Kristallografiya **14**, 404 (1969) [Sov. Phys. Crystallogr. **14**, 333 (1969)].
[20] F.J. Pinski *et al.*, Phys. Rev. Lett. **66**, 766 (1991).
[21] G.M. Stocks and W.H. Butler, Phys. Rev. Lett. **48**, 55 (1982).
[22] W. Kohn, Phys. Rev. Lett. **2**, 393 (1959).
[23] H. Sato and R.S. Toth, Phys. Rev. **127**, 469 (1962).
[24] S.C. Moss, Phys. Rev. Lett. **22**, 1108 (1969).
[25] L. Reinhard, B. Schönfeld, G. Kostorz, and W. Bührer, Phys. Rev. B **41**, 1727 (1990).
[26] G. Ceder *et al.*, Phys. Rev. B **49**, 1 (1994).
[27] J. Vrijen, P.M. Bronsveld, J. van der Veen, and S. Radelaar, Z. Metallk. **67**, 473 (1976).
[28] *Binary Alloy Phase Diagrams*, 2nd ed., edited by B. Massalski, H. Okamoto, P.R. Subramanian, and L. Kacprzak (ASM International, New York, 1990).
[29] R. Prasad, S. Papadopoulos, and A. Bansil, Phys. Rev. B **23**, 2607 (1981).
[30] G.M. Stocks *et al.*, in *Noble Metal Alloys: Phase Diagrams, Alloy Phase Stability, Thermodynamic Aspects, and Special Features*, edited by T. B. Massalski *et al.* (American Institute of Mechanical Engineers, New York, 1985).
[31] D.D. Johnson *et al.*, Phys. Rev. B **41**, 9701 (1990).
[32] D.D. Johnson and F.J. Pinski, Phys. Rev. B **48**, 11 553 (1993).
[33] M. Sluiter *et al.*, in *Neutron Scattering for Materials Science*, edited by S. Shapiro, S. Moss, and J. Jorgensen (Materials Research Society, The Netherlands, 1990), Vol. 166.
[34] P.E.A. Turchi *et al.*, Phys. Rev. Lett. **67**, 1779 (1991).
[35] V.L. Moruzzi, J.F. Janak, and A.R. Williams, *Calculated Electronic Properties of Metals* (Pergamon Press, New York, 1978).
[36] Neil W. Ashcroft and N. David Mermin, *Solid State Physics* (Saunders College, Philadelphia, 1976).
[37] J. Clark *et al.*, Phys. Rev. Lett. **74**, 3225 (1995).
[38] J.B. Cohen, J. Mater. Sci. **4**, 1012 (1969).
[39] D.D. Johnson (unpublished).
[40] F. Ducastelle and F. Gautier, J. Phys. F **6**, 2039 (1976).
[41] F. Gautier, F. Ducastelle, and J. Giner, Philos. Mag. **31**, 1373 (1975).
[42] S.C. Moss (unpublished).
[43] H. Thomas, Z. Metallk. **63**, 106 (1977).
[44] D. de Fontaine, J. Phys. Chem. Solids **34**, 1285 (1973).